BJR

https://doi.org/10.1259/bjr.20180019

Received: 28 December 2017 | Revised: 27 March 2018 | Accepted: 11 April 2018

Cite this article as:
Kiefer LS, Fabian J, Lorbeer R, Machann J, Storz C, Kraus MS, et al. Inter- and intra-observer variability of an anatomical landmark-based, manual segmentation method by MRI for the assessment of skeletal muscle fat content and area in subjects from the general population. *Br J Radiol* 2018; **91**: 20180019.

THE ROLE OF IMAGING IN OBESITY SPECIAL FEATURE: FULL PAPER

Inter- and intra-observer variability of an anatomical landmark-based, manual segmentation method by MRI for the assessment of skeletal muscle fat content and area in subjects from the general population

[1]LENA SOPHIE KIEFER, MD, [1]JANA FABIAN, BS, [2]ROBERTO LORBEER, PhD, [3,4,5]JÜRGEN MACHANN, PhD, [1]CORINNA STORZ, MD, [1]MAREEN SARAH KRAUS, MD, [6]ELKE WINTERMEYER, MD, [7]CHRISTOPHER SCHLETT, MD, MPH, [8]FRANK ROEMER, MD, [1]KONSTANTIN NIKOLAOU, MD, [9,10,11]ANNETTE PETERS, PhD and [1,9]FABIAN BAMBERG, MD, MPH

[1]Department of Diagnostic and Interventional Radiology, University of Tuebingen, Tuebingen, Germany
[2]Department of Radiology, Ludwig-Maximilian-University Hospital, Munich, Germany
[3]Department of Diagnostic and Interventional Radiology, Section of Experimental Radiology, University of Tuebingen, Tuebingen, Germany
[4]Institute for Diabetes Research and Metabolic Diseases (IDM) of the Helmholtz Center Munich at the University of Tuebingen, Tuebingen, Germany
[5]German Center for Diabetes Research (DZD), Neuherberg, Germany
[6]BG Trauma Center, University of Tuebingen, Tuebingen, Germany
[7]Department of Radiology, Diagnostic and Interventional Radiology, University of Heidelberg, Heidelberg, Germany
[8]Department of Radiology, University of Erlangen-Nuremberg, Erlangen, Germany
[9]German Center for Cardiovascular Disease Research (DZHK e.V.), Munich, Germany
[10]Institute for Cardiovascular Prevention, Ludwig-Maximilian-University-Hospital, Munich, Germany
[11]Institute of Epidemiology II, Helmholtz Zentrum Munich, German Research Center for Environmental Health, Neuherberg, Germany

Address correspondence to: Professor Fabian Bamberg
E-mail: *fabian.bamberg@uni-tuebingen.de*

Objectives: Changes in skeletal muscle composition, such as fat content and mass, may exert unique metabolic and musculoskeletal risks; however, the reproducibility of their assessment is unknown. We determined the variability of the assessment of skeletal muscle fat content and area by MRI in a population-based sample.

Methods: A random sample from a prospective, community-based cohort study (KORA-FF4) was included. Skeletal muscle fat content was quantified as proton-density fat fraction (PDFF) and area as cross-sectional area (CSA) in multi-echo Dixon sequences (TR 8.90 ms, six echo times, flip angle 4°) by a standardized, anatomical landmark-based, manual skeletal muscle segmentation at level L3 vertebra by two independent observers. Reproducibility was assessed by intraclass correlation coefficients (ICC), scatter and Bland–Altman plots.

Results: From 50 subjects included (mean age 56.1 ± 8.8 years, 60.0% males, mean body mass index 28.3 ± 5.2) 2'400 measurements were obtained. Interobserver agreement was excellent for all muscle compartments (PDFF: ICC0.99, CSA: ICC0.98) with only minor absolute and relative differences (−0.2 ± 0.5%, 31 ± 44.7 mm^2; −2.6 ± 6.4% and 2.7 ± 3.9%, respectively). Intra-observer reproducibility was similarly excellent (PDFF: ICC1.0, 0.0 ± 0.4%, 0.4%; CSA: ICC1.0, 5.5 ± 25.3 mm^2, 0.5%, absolute and relative differences, respectively). All agreement was independent of age, gender, body mass index, body height and visceral adipose tissue (ICC0.96–1.0). Furthermore, PDFF reproducibility was independent of CSA (ICC0.93–0.99).

Conclusions:
Quantification of skeletal muscle fat content and area by MRI using an anatomical landmark-based, manual skeletal muscle segmentation is highly reproducible.

Advances in knowledge: An anatomical landmark-based, manual skeletal muscle segmentation provides high reproducibility of skeletal muscle fat content and area and may therefore serve as a robust proxy for myosteatosis and sarcopenia in large cohort studies.

INTRODUCTION

Skeletal muscle represents an essential organ system, determining the physical condition and serving locomotion, physical activity and mobility, but also playing a crucial role in energy metabolism and hormone homeostasis.[1,2] It may therefore serve as an ideal target for health preservation and/or improvement.[3,4] In fact, changes in skeletal muscle composition, for example, an increase in intra- and intermuscular fat defined as myosteatosis[5] or a decline in skeletal muscle mass and performance,[6] are associated with various chronic disease conditions, such as diabetes mellitus (DM) or sarcopenia.[7–11] With more than 833 million people worldwide being affected by DM and its precursor stage prediabetes[12] and an estimated prevalence of sarcopenia up to 50% for patients aged 80 years and older,[6] the socioeconomic impact of both entities is substantial but interactions are still not well understood.

Since skeletal muscle is a major target organ of insulin, recent data suggest that patients with DM are at high risk for skeletal muscle depletion.[11] Specifically, Type 2 diabetes mellitus (T2DM) is associated with an increased prevalence of sarcopenia, defined as a decline in skeletal muscle mass associated with impaired mobility and physical disability,[6] while myosteatosis has been identified as an effect modifier in DM.[11,13–18] Despite these early data, it remains unclear to what extent ectopic lipid deposits in skeletal muscle contribute to the development and progression of insulin resistance and, conversely, how T2DM is associated with the successive loss of skeletal muscle mass, strength and function. Hence, large, longitudinal cohort studies are needed to gain profound insights into the pathophysiological relevance of myosteatosis and sarcopenia and their correlation with DM as potential diagnostic or prognostic biomarkers.

For this purpose MRI may be particularly suited to analyze skeletal muscle composition, considering its high soft tissue contrast, non-ionizing and non-invasive nature.[19–22] The feasibility of such an approach relies on a robust method for the quantification of skeletal muscle biomarkers, such as fat content and mass. However, the reproducibility of the assessment of skeletal muscle fat content and area by MRI in a cohort setting remains unknown.

We therefore aimed to determine the reproducibility of the MR-based quantification of skeletal muscle fat content and area using an anatomical landmark-based, manual segmentation approach in a sample from the general population. Our hypothesis was that such an approach will be robust and highly reproducible and may therefore serve as a reference for future studies.

METHODS AND MATERIALS

Study design and population

Subjects were derived from the KORA-FF4 study (2013–2014, n = 1851), a 14-year follow-up study of the Cooperative Health Research in the Region of Augsburg (KORA) survey S4 (1999–2001, n = 4261). The design of the KORA studies has been described in detail previously.[23,24] In brief, the KORA study was designed as a case–control study embedded in a prospective, population-based cohort including participants with normal glucose tolerance, prediabetes and T2DM from the general population. The study was approved by the local institutional review board of the Ludwig-Maximilian-University Munich, and written informed consent was obtained from all participants. Subjects underwent a whole-body MRI according to the following inclusion (willingness to undergo MRI examination, signed informed consent form) and exclusion criteria (age >72 years, validated/self-reported history of stroke, myocardial infarction or revascularization, cardiac pacemaker or implantable defibrillator, cerebral aneurysm clip, neural stimulator, any type of ear implant, ocular foreign body, any implanted device, pregnant or breast-feeding female subjects, claustrophobia, allergy against gadolinium compounds, serum creatinine ≥1.3 mg dl^{-1}).

MR imaging protocol and data acquisition

MR examinations were performed in supine position on a 3-Tesla Magnetom Skyra (Siemens Healthineers, Erlangen, Germany) using an 18-channel body surface coil in combination with the table-mounted spine matrix coil. The complete imaging protocol as well as technical specifications have been described in detail elsewhere.[24]

The imaging protocol included a T_2*-corrected, multi-echo 3D-gradient-echo Dixon-based sequence (multi-echo Dixon), originally determined for liver fat quantification[25,26] but also suited for the measurement of skeletal muscle fat content and area.[19–22] This multi-echo Dixon method is based on a prototype VIBE sequence with the following parameters: time to repetition (TR) 8.90 ms, time to echo (TEs) opposed-phase 1.23 ms, 3.69 ms and 6.15 ms, TEs in-phase 2.46 ms, 4.92 ms and 7.38 ms, flip angle 4°, readout echo bandwidth 1080 Hz/pixel, matrix 256 × 256, slice thickness 4 mm. Data were acquired during a single breath-hold of 15 s. The post-processing algorithm using the Software LiverLab (Version VD13, Siemens Healthineers, Cary, USA) automatically calculated water- and fat-only images as DICOM files from the original data of the multi-echo acquisitions. As chemical shift-based imaging, the obtained fat signal fraction maps are based on the signal ratio of fat to the summed signal of water and fat (proton-density fat fraction (PDFF)) and corrected for confounding effects of T1- and T2*-decay, quantitatively coding the mean PDFF in degrees of grey values of each voxel (1 grey value = 0.1% fat content).[25,26] Furthermore, for the correct location of L3 vertebra on axial slices, coronal two-point Dixon gradient-echo (GRE) sequences (TR 4.06 ms, TE 1.26 ms and 2.49 ms, flip angle 9°, slice thickness 1.7 mm, isotropic in-plane resolution 1.7 mm) were used.

Skeletal muscle segmentation

To determine the interobserver reproducibility, two blinded observers (observer A and observer B) independently performed skeletal muscle segmentation of 50 randomly selected KORA-data sets. For the assessment of intra-observer reproducibility, observer A repeated the segmentation of all 50 data sets in a random order at least 4 weeks after the first reading in order to reduce recall bias. All analyses were performed in a blinded manner, unaware of any information or clinical covariates of the subjects. Standard display settings were chosen to maximize

Figure 1. Skeletal muscle mass area by CSA. High (a) and low (b) skeletal muscle mass area as CSA by an anatomical landmark-based, manual segmentation method at level L3 vertebra. CSA, cross-sectional area.

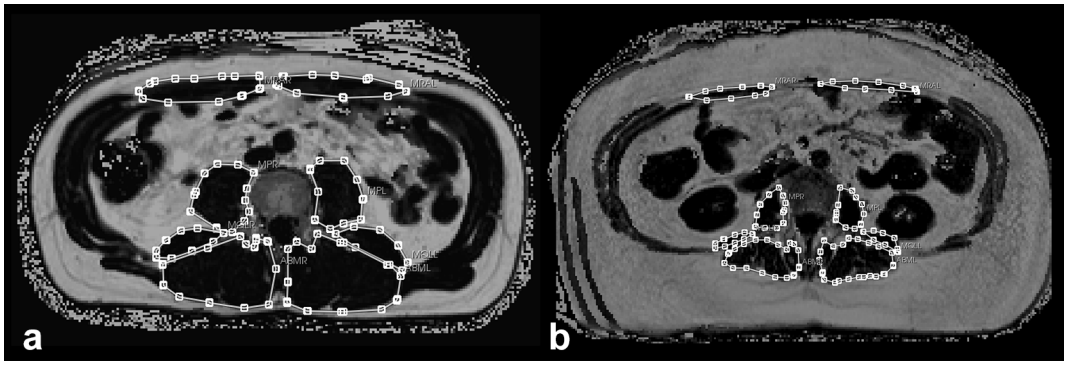

the contrast between skeletal muscle and surrounding tissue. If necessary, the observers made manual adjustments for the best image contrast. Both readers had full access to scroll through all image data sets.

Observer A and observer B both measured skeletal muscle fat content as mean PDFF in percent (%) and skeletal muscle area as muscle cross-sectional area (CSA) in square millimeters (mm^2) of the right (R) and left (L) psoas major muscle (MPM), quadratus lumborum muscle (MQL), autochthonous back muscles (ABM, containing the erector spinae muscles and the spinotransverse muscles) and rectus abdominis muscle (MRA) using dedicated, commercially available Software (Osirix V8.5.1, Pixmeo SARL, Bernex, Switzerland and MITK V2015.5.2, German Cancer Research Center, Heidelberg, Germany, respectively) on an offline workstation (Figures 1 and 2b). The validity of these methods has been demonstrated previously.[19,20,27,28] The complete manual segmentation procedure of one KORA-data set measuring both PDFF and CSA took on average 10 min.

Segmentation was performed on one axial slice at the level of the lower endplate of L3 vertebra, since recent studies demonstrated that skeletal muscle CSA at level L3 is a reliable method for the determination of sarcopenia[28] and quantification of skeletal muscle fat content at level L4 and L3 vertebra are good surrogates for the entire lumbar spine.[29] The correct axial slice position was verified by identifying L4 vertebra by the iliac crest tangent sign on coronal images using cross-reference (Figure 2).[30] If there were significant image artefacts limited to level L3 vertebra, the next possible, cranial slice without artifacts, was selected for skeletal muscle segmentation.

Each muscle compartment was segmented by a standardized and manual segmentation method on the selected axial slice. Regions of interest (ROIs) determining CSA were drawn exactly on the muscle boundaries, comprising the whole muscle area, whereas ROIs quantifying PDFF were drawn a few voxels smaller concentrically in order to avoid partial volume effects of surrounding adipose tissue. Dedicated and standardized anatomical

Figure 2. Determination of the correct axial slice position at the level of the lower endplate of L3 vertebra and skeletal muscle fat content by PDFF. Iliac crest tangent sign on coronal images, marking either L4 vertebra or L4/5 intervertebral disc and cross-reference to axial images for the identification of level L3 vertebra (a and b). Mean skeletal muscle fat content as mean PDFF in one ROI at level L3 vertebra (b). PDFF, proton-density fat fraction; ROI, region of interest.

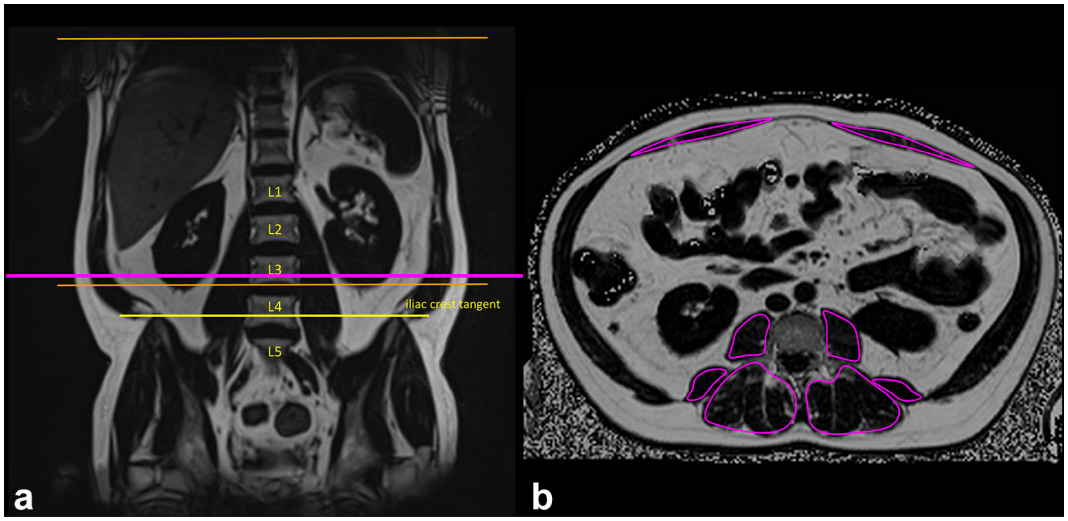

landmarks were used to define the boundaries of the segmented muscle compartments (Supplementary table 1).

Covariates

A comprehensive health assessment was performed prospectively for all subjects collecting demographics and other cardiovascular risk factors. In this analysis, we included gender, age in years, body weight measured in kilograms (kg) and body height measured in centimeters (cm). The body mass index (BMI) was calculated as weight in kg divided by height in square meters (m^2). Waist circumference was measured at the smallest abdominal circumference or, in obese subjects, in the midpoint of the lowest rib and the upper margin of the iliac crest and hip circumference was determined at the most protruding part of the hips to the nearest 1 mm. In addition, visceral and subcutaneous adipose tissue (VAT and SCAT) were segmented and quantified in cm^2 by an automated algorithm based on fuzzy-clustering on one axial slice at the level of the umbilicus.[31,32]

Statistical analysis

Descriptive characteristics were expressed as mean ± standard deviation (SD) for continuous variables and percentages for categorical variables. Inter- and intra-observer reproducibility was assessed using scatter plots with Pearson correlation coefficients and intraclass correlation coefficients (ICC) from two-way random-effects ANOVA[33] as well as Bland–Altman plots with mean absolute differences ± SD and 95% limits of agreement. In addition, relative differences between the two observers were calculated and presented as mean ± SD. An ICC value close to 1 indicates excellent agreement between the two observers or observations. Analyses were repeated in subgroups (median divided) of age, gender, BMI, body height, VAT and CSA. All statistical analysis was performed using Stata (V14.1, Stata Corporation, College Station, USA).

RESULTS

Study population

A total of 50 randomly selected subjects from the entire KORA-MRI study population were included in this analysis (mean age 56.1 ± 8.8 years, 60.0% males, mean BMI 28.3 ± 5.2). No subject was excluded due to impaired image quality. Segmentation had to be performed at level L2/3 vertebra in four subjects (8%) due to image artefacts limited to level L3. Demographics of the study population are provided in Table 1). For the assessment of inter- and intra-observer reproducibility of PDFF and CSA consequently a total of 1'200 measurements each were obtained.

Inter-observer reproducibility

The interobserver agreement of PDFF was excellent for all muscle compartments (ICC 0.94 to 1.0) (Table 2). Similarly, inter-observer reproducibility of CSA was excellent for all included muscles (ICC 0.93 to 0.97) (Table 3). PDFF and CSA measurements were both highly correlated between the two separate measurements by observer A and B (r = 0.99, ICC 0.99 and r = 0.99, ICC 0.98, respectively, Figures 3 and 4) with only minor mean absolute differences (mean absolute differences PDFF: −0.2 ± 0.5% and CSA: 31.0 ± 44.7 mm^2, respectively). The mean variability was likewise very small for PDFF and CSA (mean relative difference PDFF: −2.6 ± 6.4% and CSA: 2.7±3.9%, respectively) (Tables 2 and 3).

Intra-observer reproducibility

For all analyzed muscle compartments, intra-observer reproducibility was excellent regarding PDFF (ICC 0.96 to 1.0) and CSA (ICC 0.96 to 0.98) (Tables 2 and 3). PDFF and CSA measurements were highly correlated between the first and second reading by the same observer A (r = 1.00, ICC 1.00 each, Figures 5 and 6). The mean absolute and relative intra-observer differences were extremely small for both PDFF and CSA (mean absolute differences PDFF: 0.0±0.4% and CSA: 5.5 ± 25.3 mm^2; mean relative differences PDFF: 0.4±3.8% and CSA: 0.5±2.3%; respectively) (Tables 2 and 3).

Effects of age, gender, BMI, body height, VAT and skeletal muscle mass on reproducibility

All agreement of PDFF and CSA was independent of age (PDFF: ICC 0.98 to 0.99 and CSA: ICC 0.97 to 1.0), gender (PDFF: ICC 0.99 to 1.0 and CSA: ICC 0.96 to 0.99), BMI (PDFF: ICC 0.98 to 1.0 and CSA: ICC 0.97 to 1.0), body height (PDFF: ICC 0.97 to 1.0 and CSA: ICC 0.97 to 0.99) and VAT (PDFF: ICC 0.99 to 1.0 and CSA: ICC 0.96 to 1.0) (Supplementary Table 1 and

Table 1. Demographics of the study population. Data is presented as mean ± standard deviation

Characteristics	All subjects	Female	Male
N	50	20	30
Age (years)	56.1 ± 8.8	56.7 ± 9.5	55.8 ± 8.4
BMI (kg/m^2)	28.3 ± 5.2	27.8 ± 6.4	28.5 ± 4.2
Body weight (kg)	83.8 ± 17.3	75.8 ± 18	89.2 ± 14.8
Body height (cm)	172.0 ± 9.3	165.1 ± 6.6	176.6 ± 7.8
Waist circumference (cm)	97.9 ± 14.5	90.1 ± 15.3	103.1 ± 11.5
Hip circumference (cm)	106.7 ± 10	107.4 ± 12.8	106.2 ± 7.7
VAT (cm^2)	156.1 ± 95	100.8 ± 64.9	193.7 ± 94.6
SCAT (cm^2)	290.4 ± 123.1	318.5 ± 154.4	271.4 ± 94.8

BMI, body mass index; VAT, visceral adipose tissue; SCAT, subcutaneous adipose tissue

Table 2. Inter- and intra-observer reproducibility of PDFF

	Interobserver variability PDFF			Intra-observer variability PDFF		
	ICC (95% CI)	Difference (mean ± SD)		ICC (95% CI)	Difference (mean ± SD)	
		Absolute (%)	Relative (%)		Absolute (%)	Relative (%)
Psoas major muscle (right)	0.94 (0.89;0.97)	−0.3 ± 0.9	−3.7 ± 13.6	0.96 (0.93;0.98)	0.1 ± 0.8	1.4 ± 12.0
Psoas major muscle (left)	0.98 (0.97;0.99)	−0.2 ± 0.6	−2.1 ± 9.3	0.98 (0.97;0.99)	−0.1 ± 0.5	0.2 ± 9.3
Quadratus lumborum muscle (right)	0.97 (0.96;0.99)	0.1 ± 0.7	2.6 ± 16.7	0.98 (0.96;0.99)	0.1 ± 0.7	1.8 ± 14.7
Quadratus lumborum muscle (left)	0.94 (0.9;0.97)	−0.1 ± 0.8	0.4 ± 17.6	0.98 (0.96;0.99)	0.1 ± 0.5	1.4 ± 10.7
Autochthonous back muscles (right)	0.98 (0.96;0.99)	−0.6 ± 1.5	−3.4 ± 10.9	0.99 (0.98;0.99)	−0.2 ± 1.2	−1.1 ± 7.2
Autochthonous back muscles (left)	0.99 (0.98;0.99)	−0.3 ± 1.3	−2.4 ± 8.7	0.99 (0.99;1.0)	0.3 ± 1.0	1.9 ± 7.1
Rectus abdominis muscle (right)	1.0 (0.99;1.0)	−0.4 ± 1.4	−5.9 ± 17.3	1.0 (0.99;1.0)	0.1 ± 1.5	−1.3 ± 10.8
Rectus abdominis muscle (left)	0.99 (0.98;0.99)	−0.2 ± 1.4	−2.8 ± 14.4	0.99 (0.97;0.99)	−0.2 ± 1.5	−0.1 ± 13.2
Mean skeletal muscle (bilaterally)	0.99 (0.98;1.0)	−0.2 ± 0.5	−2.6 ± 6.4	1.0 (0.99;1.0)	0.0 ± 0.4	0.4 ± 3.8

CI, confidence interval; ICC, intraclass correlation coefficient; PDFF, proton-density fat fraction.

Supplementary Table 3). The mean differences of PDFF and CSA were similar between younger subjects (<55 years), male gender, non-obese subjects (BMI <28.0 and VAT <148.4 cm^2) or subjects with a smaller body height (<171.0 cm) (for all ICC > 0.96). Furthermore, reproducibility of PDFF was independent of CSA (ICC 0.93 to 0.99).

DISCUSSION

Given the substantial impact of DM in the context of demographic change and successively increasing prevalence as well as the highly relevant functional aspects and clinical significance of skeletal muscle, there is a rising need for the establishment of reliable and robust biomarkers for myosteatosis and sarcopenia. Thus, we studied the reproducibility of the assessment of abdominal skeletal muscle fat content and area by MRI in a population-based sample. Our results indicate that both PDFF and CSA by MRI are highly reproducible using a standardized, multi-echo Dixon-based, manual segmentation method. Measurement variabilities were independent of potential confounders, such as age, gender, BMI, body height and VAT as well as of each other.

Currently, several different methods are being used for the analysis of skeletal muscle composition, including CT, dual-energy X-ray absorptiometry, ultrasound or histopathology.[34,35] However, disadvantages are the application of ionizing radiation for X-ray-based methods or the invasiveness in biopsy-based approaches. Recent studies demonstrated that multi-echo Dixon-based and spectroscopic fat fractions agree well, thus providing a valid and fast method for the quantification of skeletal muscle

Table 3. Inter- and intra-observer reproducibility of CSA

	Interobserver variability CSA			Intra-observer variability CSA		
	ICC (95% CI)	Difference (mean ± SD)		ICC (95% CI)	Difference (mean ± SD)	
		Absolute (mm^2)	Relative (%)		Absolute (mm^2)	Relative (%)
Psoas major muscle (right)	0.93 (0.88;0.96)	19.5 ± 105.0	2.5 ± 8.6	0.98 (0.97;0.99)	2.4 ± 47.8	−0.1 ± 6.0
Psoas major muscle (left)	0.97 (0.94;0.98)	7.0 ± 66.8	0.6 ± 8.1	0.97 (0.95;0.98)	10.5 ± 60.9	0.6 ± 7.0
Quadratus lumborum muscle (right)	0.95 (0.92;0.97)	13.0 ± 59.2	2.6 ± 18.5	0.97 (0.96;0.99)	4.2 ± 44.9	1.0 ± 10.7
Quadratus lumborum muscle (left)	0.96 (0.93;0.98)	2.5 ± 49.4	1.7 ± 14.0	0.97 (0.94;0.98)	−15.7 ± 40.8	−4.6 ± 11.1
Autochthonous back muscles (right)	0.97 (0.94;0.99)	58.3 ± 118	2.2 ± 5.1	0.98 (0.97;0.99)	2.8 ± 108.8	0.2 ± 4.4
Autochthonous back muscles (left)	0.97 (0.94;0.98)	33.3 ± 132.1	1.2 ± 5.4	0.98 (0.97;0.99)	22 ± 95.4	1.0 ± 3.5
Rectus abdominis muscle (right)	0.93 (0.57;0.98)	72.2 ± 70.0	10.7 ± 11.6	0.96 (0.94;0.98)	15.9 ± 74.8	3.2 ± 11.7
Rectus abdominis muscle (left)	0.95 (0.89;0.97)	41.9 ± 93.0	5.2 ± 12.3	0.98 (0.97;0.99)	1.8 ± 59.1	0.5 ± 9.3
Mean skeletal muscle (bilaterally)	0.98 (0.93;0.99)	31 ± 44.7	2.7 ± 3.9	1.0 (0.99;1.0)	5.5 ± 25.3	0.5 ± 2.3

CI, confidence interval; CSA, cross-sectional area; ICC, intraclass correlation coefficient;

Figure 3. Interobserver correlation of PDFF. (a) Scatter plot of the PDFF inter-observer correlation demonstrating the linear correlation between observer A and observer B (r = 0.99, ICC = 0.99). (b) Bland–Altman plot demonstrating a mean difference of −0.249 (CI −0.396 to −0.102). PDFF, proton-density fat fraction.

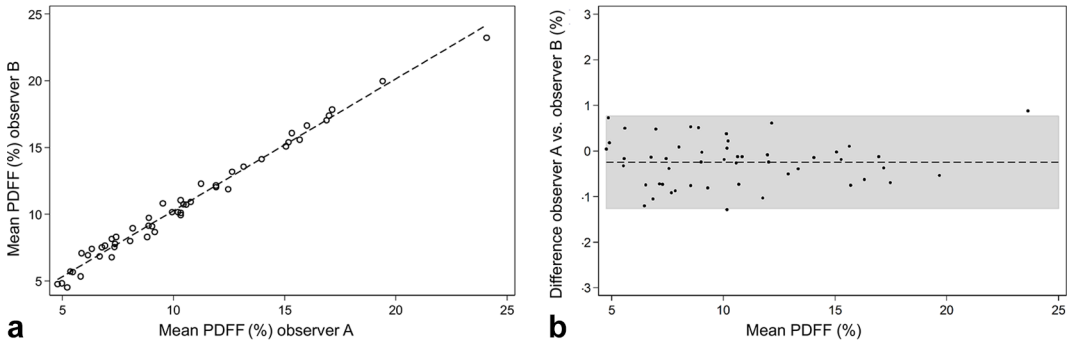

fat content.[20] Hence, chemical-shift MRI, as used in this study, is considered the contemporary standard for the evaluation of skeletal muscle composition, structure and mass providing reliable measurements also for minor changes.[19–22] However, the reliability of an MRI-based assessment of skeletal muscle parameters in a larger cohort setting using a standardized approach based on distinct anatomical landmarks of the lumbar spine remains unknown.

We extend earlier observations of the high reproducibility of PDFF measurements in the supraspinatus muscle.[19] In this study, Agten et al found that quantification of fat content in the supraspinatus muscle by multi-echo Dixon is a reliable method and is comparable to MR spectroscopy. Similar to our approach, their results indicate substantial to almost perfect inter- and intra-observer agreement of PDFF measurements (ICC 0.76 to 0.89). Their approach was similarly based on chemical-shift MRI and sample ROI PDFF quantification of the entire muscle CSA.

Furthermore, our results agree well with recent CT-based evaluations by Jones et al, reporting good interobserver reproducibility of psoas muscle CSA as a reliable marker for sarcopenia using non-enhanced CT acquisitions (r^2 = 0.97, 95% CI 0.89 to 0.98, p = 0.001), although the study population consisted of oncological patients undergoing elective resection of colorectal carcinoma.[28] Our findings confirm prior results that an imaging-based assessment of skeletal muscle composition may be considered as a reliable biomarker and extend these observations to MRI, which may be particularly suited for asymptomatic subjects.

Regarding the assessment of skeletal muscle fat content, the applied anatomical landmark-based approach takes into account that extramyocellular-intrafascial adipose tissue may exert specific metabolic and structural functions and could potentially compromise the functional capacity of myocytes and muscle tissue.[36] Thus, extramyocellular-extramyofascial adipose tissue adjacent to muscle tissue has to be separated accurately from intrafascial adipose tissue and should therefore be excluded from skeletal muscle composition analysis. Since recent studies have emphasized the functional properties of skeletal muscle and skeletal muscle adipose tissue as an endocrine organ, further studies will have to discriminate the different properties of intra- and intermyocellular-intrafascial lipids and adipose tissue regarding different metabolic and musculoskeletal disorders.

It is well known that abdominal skeletal muscle compartments differ regarding muscle fiber-type composition and function. Hence, it is important to include both predominantly oxidative, fiber-type l containing muscles, such as the autochthonous back muscles with their mainly postural function, and predominantly glycolytic, fiber-type llA containing muscles, such as the psoas major, with its dynamic function as a flexor of the hip joint.[37,38]

Figure 4. Interobserver correlation of CSA. (a) Scatter plot of the CSA inter-observer correlation demonstrating the linear correlation between observer A and observer B (r = 0.99, ICC = 0.98). (b) Bland–Altman plot demonstrating a mean difference of 30.959 (CI 18.242 to 43.676). CSA, cross-sectional area.

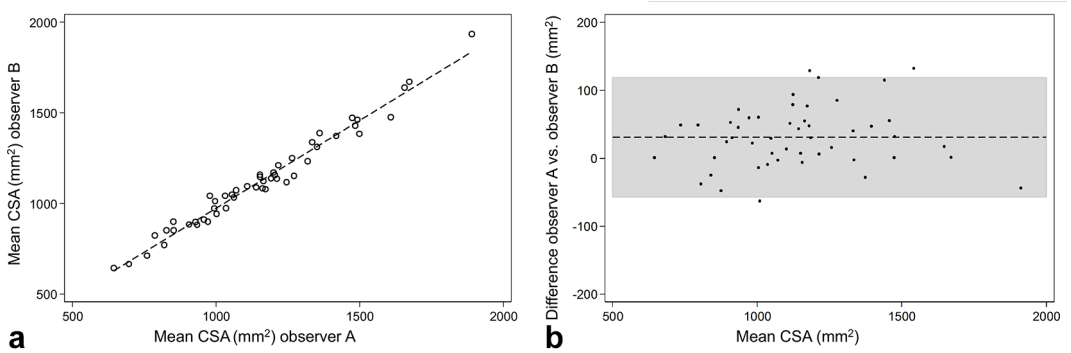

Figure 5. Intra-observer correlation of PDFF. (a) Scatter plot of the PDFF intra-observer correlation demonstrating the linear correlation between the first and second observing by observer A (r = 1.00, ICC 1.00). (b) Bland–Altman plot demonstrating a mean difference of 0.018 (CI −0.097 to 0.132). PDFF, proton-density fat fraction.

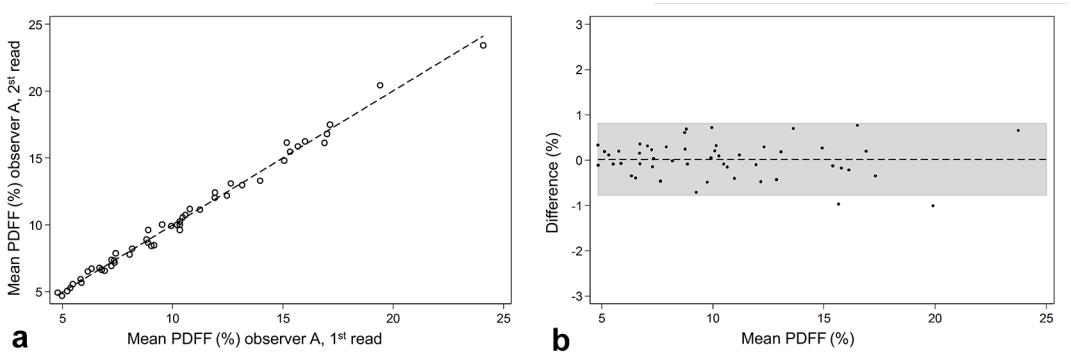

Since different muscle fiber-types exhibit different insulin sensitivity and have a variable amount of fat content and T2DM is characterized by a decrease of oxidative type I and an increase of glycolytic Type II muscle fibers,[39] further studies will have to focus on the composition of abdominal skeletal muscle compartments and its DM-related change.

As a consequence, both PDFF and CSA as distinct skeletal muscle parameters may serve as reliable biomarkers for skeletal muscle fat content and area and their assessment may therefore be implemented also in large, population-based cohort studies. Two current examples are the German National Cohort[40] and the imaging enhancement program of the UK Biobank.[41] As part of those and other ongoing studies, the value of these biomarkers in a socioeconomic and potentially clinical context will have to be determined. Besides the potential risk-related value in healthy and asymptomatic subjects, these parameters might also be relevant in distinct patient populations, for instance, in perioperative risk evaluation. However, while the method itself may be robust, its clinical implications will need to be determined. Furthermore, given the high prevalence of DM and sarcopenia, future research should analyze potential correlations, comorbidities and complications of both diseases based on the standardized approach evaluated in this study.

Our study has some limitations. First, this study is focused on the inter- and intra-observer agreement of skeletal muscle parameters determining observer and observing differences and not comparing the results to a gold standard, such as histopathology for skeletal muscle fat content or dual-energy X-ray absorptiometry for skeletal muscle mass. However, former studies have demonstrated the validity of the PDFF and CSA quantification methods used in this study.[20,28] Second, our approach for the quantification of skeletal muscle fat content and area was based on manual segmentation. This may limit the application possibility, particularly with regard to very large cohort settings. Therefore, more advanced post-processing techniques implemented within image analysis pipelines, for example automatic or semiautomatic segmentation tools trained by a reference standard of quality-controlled manual segmentation, will be necessary. Since manual segmentation is still considered the gold standard for segmentation approaches in general, segmentation data from this study may be used as training data to implement a reference standard.[42,43] Third, due to the design of this study, we did not specifically study subjects with established myosteatosis and/or sarcopenia, which may have introduced significant selection bias. However, since we included subjects from a population-based sample potentially suffering from myosteatosis and/or sarcopenia as prevalent in the general population and while the reproducibility of their

Figure 6. Intra-observer correlation of CSA. (a) Scatter plot of the CSA intra-observer correlation demonstrating the linear correlation between the first and second observing by observer A (*r* = 1.00, ICC = 1.00). (b) Bland–Altman plot demonstrating a mean difference of 5.490 (CI −1.702 to −12.682). CSA, cross-sectional area.

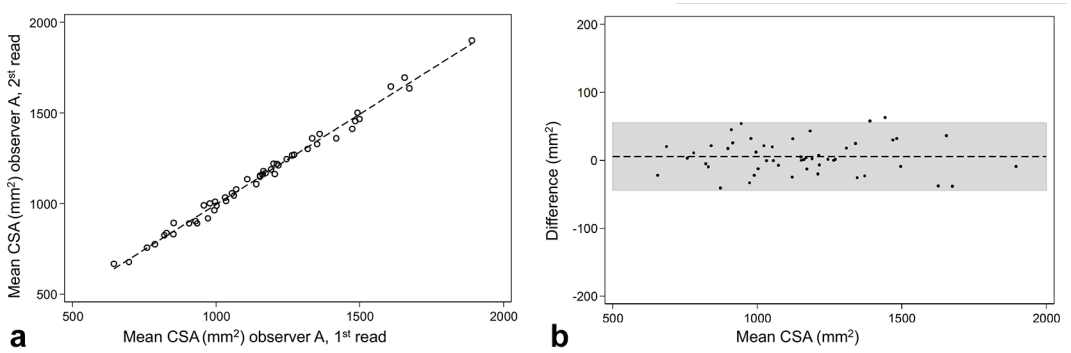

measurement method is particularly relevant in subjects from the general population with potentially milder forms of adipose tissue accumulation and loss of skeletal muscle mass, further confirmation in subjects with established conditions is warranted. Fourth, sample ROI measurements on one single axial slice at level L3 vertebra, as performed in this study, may not reproduce a heterogeneous distribution of skeletal muscle fat and area within the entire muscle due to undersampling. However, recent studies showed that level L4 and L3 vertebra are representative for the entire lumbar spine.[28,29] A single level-based PDFF and CSA measurement may therefore represent a valid and cost-effective approach to the assessment of skeletal muscle fat content and area as a free by-product in hepatic or abdominal MRI examinations.

CONCLUSIONS

Quantification of skeletal muscle parameters, such as skeletal muscle fat content and area, using a standardized, anatomical landmark-based, manual segmentation of multi-echo Dixon MRI-data sets provides excellent inter- and intra-observer reproducibility. Thus, these parameters may serve as robust and reliable biomarkers, particularly in large and longitudinal cohort studies, providing new insights into the role of skeletal muscle in different disease states and potentially enhance metabolic and musculoskeletal risk stratification in healthy, asymptomatic and symptomatic subjects.

ACKNOWLEDGEMENT

This study was funded by the German Research Foundation (DFG, Bonn, Germany), the German Centre for Cardiovascular Disease Research (DZHK, Berlin, Germany) and the Centre for Diabetes Research (DZD e.V., Neuherberg, Germany).

REFERENCES

1. Iizuka K, Machida T, Hirafuji M. Skeletal muscle is an endocrine organ. *J Pharmacol Sci* 2014; **125**: 125–31. doi: https://doi.org/10.1254/jphs.14R02CP
2. Giudice J, Taylor JM. Muscle as a paracrine and endocrine organ. *Curr Opin Pharmacol* 2017; **34**: 49–55. doi: https://doi.org/10.1016/j.coph.2017.05.005
3. Warburton DER, Nicol CW, Bredin SSD. Health benefits of physical activity: the evidence. *Can Med Assoc J* 2006; **174**: 801–9. doi: https://doi.org/10.1503/cmaj.051351
4. Ding D, Lawson KD, Kolbe-Alexander TL, Finkelstein EA, Katzmarzyk PT, van Mechelen W, et al.Lancet Physical Activity Series 2 Executive Committee The economic burden of physical inactivity: a global analysis of major non-communicable diseases. *Lancet* 2016; **388**: 1311–24. doi: https://doi.org/10.1016/S0140-6736(16)30383-X
5. Miljkovic I, Zmuda JM. Epidemiology of myosteatosis. *Curr Opin Clin Nutr Metab Care* 2010; **13**: 260–4. doi: https://doi.org/10.1097/MCO.0b013e328337d826
6. von Haehling S, Morley JE, Anker SD. An overview of sarcopenia: facts and numbers on prevalence and clinical impact. *J Cachexia Sarcopenia Muscle* 2010; **1**: 129–33. doi: https://doi.org/10.1007/s13539-010-0014-2
7. Machann J, Häring H, Schick F, Stumvoll M. Intramyocellular lipids and insulin resistance. *Diabetes, Obesity and Metabolism* 2004; **6**: 239–48. doi: https://doi.org/10.1111/j.1462-8902.2004.00339.x
8. Jacob S, Machann J, Rett K, Brechtel K, Volk A, Renn W, et al. Association of increased intramyocellular lipid content with insulin resistance in lean nondiabetic offspring of type 2 diabetic subjects. *Diabetes* 1999; **48**: 1113–9. doi: https://doi.org/10.2337/diabetes.48.5.1113
9. Boettcher M, Machann J, Stefan N, Thamer C, Häring HU, Claussen CD, et al. Intermuscular adipose tissue (IMAT): association with other adipose tissue compartments and insulin sensitivity. *J Magn Reson Imaging* 2009; **29**: 1340–5. doi: https://doi.org/10.1002/jmri.21754
10. Volpato S, Bianchi L, Lauretani F, Lauretani F, Bandinelli S, Guralnik JM, et al. Role of muscle mass and muscle quality in the association between diabetes and gait speed. *Diabetes Care* 2012; **35**: 1672–9. doi: https://doi.org/10.2337/dc11-2202
11. Park SW, Goodpaster BH, Lee JS, Kuller LH, Boudreau R, de Rekeneire N, et al.Health, Aging, and Body Composition Study Excessive loss of skeletal muscle mass in older adults with type 2 diabetes. *Diabetes Care* 2009; **32**: 1993–7. doi: https://doi.org/10.2337/dc09-0264
12. International Diabetes Federation. *Diabetes Atlas*, IDF Diabetes Atlas 7th ed 2015. 2015.
13. Wang T, Feng X, Zhou J, Gong H, Xia S, Wei Q, et al. Type 2 diabetes mellitus is associated with increased risks of sarcopenia and pre-sarcopenia in Chinese elderly. *Sci Rep* 2016; **6**: 1–7. doi: https://doi.org/10.1038/srep38937
14. Bouchi R, Fukuda T, Takeuchi T, Nakano Y, Murakami M, Minami I, et al. Association of sarcopenia with both latent autoimmune diabetes in adults and type 2 diabetes: a cross-sectional study. *J Diabetes Complications* 2017; **31**: 992–6. doi: https://doi.org/10.1016/j.jdiacomp.2017.02.021
15. Volpato S, Blaum C, Resnick H, Ferrucci L, Fried LP, Guralnik JM, et al. Comorbidities and impairments explaining the association between diabetes and lower extremity disability: the women's health and aging study. *Diabetes Care* 2002; **25**: 678–83. doi: https://doi.org/10.2337/diacare.25.4.678
16. Brøns C, Grunnet LG. MECHANISMS IN ENDOCRINOLOGY: Skeletal muscle lipotoxicity in insulin resistance and type 2 diabetes: a causal mechanism or an innocent bystander? *Eur J Endocrinol* 2017; **176**: R67–R78. doi: https://doi.org/10.1530/EJE-16-0488
17. Miljkovic I, Kuipers AL, Cvejkus R, Bunker CH, Patrick AL, Gordon CL, et al. Myosteatosis increases with aging and is associated with incident diabetes in African ancestry men. *Obesity* 2016; **24**: 476–82. doi: https://doi.org/10.1002/oby.21328
18. Phillips A, Strobl R, Vogt S, Ladwig KH, Thorand B, Grill E, et al. Sarcopenia is associated with disability status-results from the KORA-Age study. *Osteoporos Int* 2017; **28**: 2069–79. doi: https://doi.org/10.1007/s00198-017-4027-y
19. Agten CA, Rosskopf AB, Gerber C, Pfirrmann CW. Quantification of early fatty infiltration of the rotator cuff muscles: comparison of multi-echo Dixon with single-voxel MR spectroscopy. *Eur Radiol* 2016; **26**: 3719–27. doi: https://doi.org/10.1007/s00330-015-4144-y
20. Fischer MA, Nanz D, Shimakawa A, Schirmer T, Guggenberger R, Chhabra A, et al. Quantification of muscle fat in patients

with low back pain: comparison of multi-echo MR imaging with single-voxel MR spectroscopy. *Radiology* 2013; **266**: 555–63. doi: https://doi.org/10.1148/radiol.12120399
21. Elliott JM, Courtney DM, Rademaker A, Pinto D, Sterling MM, Parrish TB, et al. The Rapid and Progressive Degeneration of the Cervical Multifidus in Whiplash: An MRI Study of Fatty Infiltration. *Spine* 2015; **40**: 395–401. doi: https://doi.org/10.1097/BRS.0000000000000891
22. Reeder SB, Hu HH, Sirlin CB. Proton density fat-fraction: A standardized mr-based biomarker of tissue fat concentration. *Journal of Magnetic Resonance Imaging* 2012; **36**: 1011–4. doi: https://doi.org/10.1002/jmri.23741
23. Holle R, Happich M, Löwel H, Wichmann H. KORA - A Research Platform for Population Based Health Research. *Gesundheitswesen* 2005; **67**(S 01): 19–25. doi: https://doi.org/10.1055/s-2005-858235
24. Bamberg F, Hetterich H, Rospleszcz S, Lorbeer R, Auweter SD, Schlett CL, et al. Subclinical disease burden as assessed by whole-body MRI in subjects with prediabetes, subjects with diabetes, and normal control subjects from the general population: The KORA-MRI study. *Diabetes* 2017; **66**: 158–69. doi: https://doi.org/10.2337/db16-0630
25. Zhong X, Nickel MD, Kannengiesser SA, Dale BM, Kiefer B, Bashir MR, et al. Liver fat quantification using a multi-step adaptive fitting approach with multi-echo GRE imaging. *Magn Reson Med* 2014; **72**: 1353–65. doi: https://doi.org/10.1002/mrm.25054
26. Bashir MR, Zhong X, Nickel MD, Fananapazir G, Kannengiesser SA, Kiefer B, et al. Quantification of hepatic steatosis with a multistep adaptive fitting MRI approach: prospective validation against MR spectroscopy. *AJR Am J Roentgenol* 2015; **204**: 297–306. doi: https://doi.org/10.2214/AJR.14.12457
27. Crawford RJ, Cornwall J, Abbott R, Elliott JM. Manually defining regions of interest when quantifying paravertebral muscles fatty infiltration from axial magnetic resonance imaging: a proposed method for the lumbar spine with anatomical cross-reference. *BMC Musculoskelet Disord* 2017; **18**: 25. doi: https://doi.org/10.1186/s12891-016-1378-z
28. Jones KI, Doleman B, Scott S, Lund JN, Williams JP. Simple psoas cross-sectional area measurement is a quick and easy method to assess sarcopenia and predicts major surgical complications. *Color. Dis* 2014; **17**: O20–O26. doi: https://doi.org/10.1111/codi.12805
29. Crawford RJ, Filli L, Elliott JM, Nanz D, Fischer MA, Marcon M, et al. Age- and level-dependence of fatty infiltration in lumbar paravertebral muscles of healthy volunteers. *AJNR Am J Neuroradiol* 2016; **37**: 742–8. doi: https://doi.org/10.3174/ajnr.A4596
30. Farshad-Amacker NA, Aichmair A, Herzog RJ, Farshad M. Merits of different anatomical landmarks for correct numbering of the lumbar vertebrae in lumbosacral transitional anomalies. *Eur Spine J* 2015; **24**: 600–8. doi: https://doi.org/10.1007/s00586-014-3573-7
31. Würslin C, Machann J, Rempp H, Claussen C, Yang B, Schick F, et al. Topography mapping of whole body adipose tissue using A fully automated and standardized procedure. *J Magn Reson Imaging* 2010; **31**: 430–9. doi: https://doi.org/10.1002/jmri.22036
32. Schwenzer NF, Machann J, Schraml C, Springer F, Ludescher B, Stefan N, et al. Quantitative analysis of adipose tissue in single transverse slices for estimation of volumes of relevant fat tissue compartments: a study in a large cohort of subjects at risk for type 2 diabetes by MRI with comparison to anthropometric data. *Invest Radiol* 2010; **45**: 788–94. doi: https://doi.org/10.1097/RLI.0b013e3181f10fe1
33. Shrout PE, Fleiss JL. Intraclass correlations: uses in assessing rater reliability. *Psychol Bull* 1979; **86**: 420–8. doi: https://doi.org/10.1037/0033-2909.86.2.420
34. Wagner DR. Ultrasound as a tool to assess body fat. *J Obes* 2013; **2013**: 280713–. doi: https://doi.org/10.1155/2013/280713
35. Lemos T, Gallagher D. Current body composition measurement techniques. *Curr Opin Endocrinol Diabetes Obes* 2017; **24**: 310–4. doi: https://doi.org/10.1097/MED.0000000000000360
36. Shahidi B, Parra CL, Berry DB, Hubbard JC, Gombatto S, Zlomislic V, et al. Contribution of Lumbar Spine Pathology and Age to Paraspinal Muscle Size and Fatty Infiltration. *Spine* 2017; **42**: 616–23. doi: https://doi.org/10.1097/BRS.0000000000001848
37. Arbanas J, Klasan GS, Nikolic M, Jerkovic R, Miljanovic I, Malnar D, et al. Fibre type composition of the human psoas major muscle with regard to the level of its origin. *J Anat* 2009; **215**: 636–41. doi: https://doi.org/10.1111/j.1469-7580.2009.01155.x
38. Mannion AF, Dumas GA, Cooper RG, Espinosa FJ, Faris MW, Stevenson JM. Muscle fibre size and type distribution in thoracic and lumbar regions of erector spinae in healthy subjects without low back pain: normal values and sex differences. *J Anat* 1997; **190**(Pt 4): 505–13. doi: https://doi.org/10.1046/j.1469-7580.1997.19040505.x
39. Oberbach A, Bossenz Y, Lehmann S, Niebauer J, Adams V, Paschke R, et al. Altered fiber distribution and fiber-specific glycolytic and oxidative enzyme activity in skeletal muscle of patients with type 2 diabetes. *Diabetes Care* 2006; **29**: 895–900. doi: https://doi.org/10.2337/diacare.29.04.06.dc05-1854
40. Bamberg F, Kauczor HU, Weckbach S, Schlett CL, Forsting M, Ladd SC, et al. Whole-body MR imaging in the German National Cohort: rationale, design, and technical background. *Radiology* 2015; **277**: 206–20. doi: https://doi.org/10.1148/radiol.2015142272
41. Sudlow C, Gallacher J, Allen N, Beral V, Burton P, Danesh J, et al. UK biobank: an open access resource for identifying the causes of a wide range of complex diseases of middle and old age. *PLoS Med* 2015; **12**: e1001779–10. doi: https://doi.org/10.1371/journal.pmed.1001779
42. Pedoia V, Majumdar S, Link TM. Segmentation of joint and musculoskeletal tissue in the study of arthritis. *Magn Reson Mater Physics Biol Med* 2016; **29**: 207–21. doi: https://doi.org/10.1007/s10334-016-0532-9
43. Gilles B, Magnenat-Thalmann N. Musculoskeletal MRI segmentation using multi-resolution simplex meshes with medial representations. *Med Image Anal* 2010; **14**: 291–302. doi: https://doi.org/10.1016/j.media.2010.01.006